IGARSS 2019 - 2019 IEEE International Geoscience and Remote Sensing Symposium, 2019
Pages 4689-4692
2019
ISBN 9781538691557
https://doi.org/10.1109/IGARSS.2019.8900538
https://archimer.ifremer.fr/doc/00706/81805/

Interpreting Surface Ocean Phenomena Through Quad-Polarized SAR Measurements

Fan Shengren [1], Kudryavtsev Vladimir [2, 3], Zhang Biao [1], Chapron Bertrand [2, 4]

[1] Nanjing Univ Informat Sci & Technol, Nanjing, Peoples R China.
[2] Russian State Hydrometeorol Univ, St Petersburg, Russia.
[3] Marine Hydrophys Inst, Sebastopol, Russia.
[4] Inst Franc Ais Rech Exploitat Mer, Issy Les Moulineaux, France.

Abstract :

RADARSAT-2 C-band quad-polarization ocean synthetic aperture radar (SAR) scenes are decomposed into resonant Bragg scattering from regular (no-breaking) surface and scattering from breaking waves. Analysis of the surface current signatures in dual co- and cross-pol SAR images revealed that governing imaging mechanism is modulations of wave breakings which are very sensitive to the presence of current non-uniformities. As found, due to small relaxation scale, short Bragg waves do not "feel" the current. Thus routinely observed current signatures in quad-pol SAR images originate essentially from wave breaking modulations, and modulation of Bragg waves does not matter this issue.

Keywords : Quad-polarization SAR scene, decompose, Bragg scattering, breaking waves

1. INTRODUCTION

The goal of this study is to further dwell on the use of high-resolution quad-polarized SAR satellite measurements to provide efficient means to interpret various surface ocean phenomena. More specifically, the polarization diversity is demonstrated to best isolate small-perturbation scattering and nonpolarized scattering associated with radar returns from steep slopes of breaking waves. As already tested [1] for a particular case-study, an effective methodology can build on using the dual co-polarization (VV and HH) radar data to interpret and quantitatively assess different detected surface ocean phenomena which include local wave breaking changes. Indeed, using polarized imagery, wave breaking is quantitatively assessed from: (1) the polarization ratio (PR), namely the ratio between the two polarizations (HH/VV); (2) the polarization difference (PD), namely the difference between VV- and HH-polarized radar signals which closely relates to the pure small-perturbation Bragg scattering; (3) the nonpolarized (NP) radar returns from breaking waves [2].

2. OBSERVATIONS AND INTERPRETATION

2.1 SAR Data

This study is based on quad-polarized RADARSAT-2 SAR images acquired over the east and west coasts of the USA, which are acquired at 14:35 UTC on August 15, 2009 (see Fig. 1) and 09:59 UTC on November 1, 2009 (see Fig. 2). A nominal image scene covers an area of approximately 25×25 km. These scenes are collected with a resolution of 8.0 m in the azimuth and 5.4 m in the range directions, covering incidence angles between 28° and 38°, from the near to far range. The pixel spacings in the azimuth and range directions are 4.73 and 4.74 m, respectively. The RADARSAT-2 fine quad-pol imaging mode provides data in HH, HV, VH, and VV polarizations. VV- and HH-polarized images are shown in Fig. 1 and 2. The corresponding image of the polarization difference (VV minus HH in linear units, hereinafter PD) are shown in Fig. 1(c) and Fig. 2(c), respectively.

In Fig. 1(a) and (b), both VV and HH SAR images exhibit distinct linear bright/dark signatures, which can be interpreted as manifestations of surface currents (front), and dark area presumably caused by the internal waves. The distinct current induced features are almost entirely removed in the PD field.

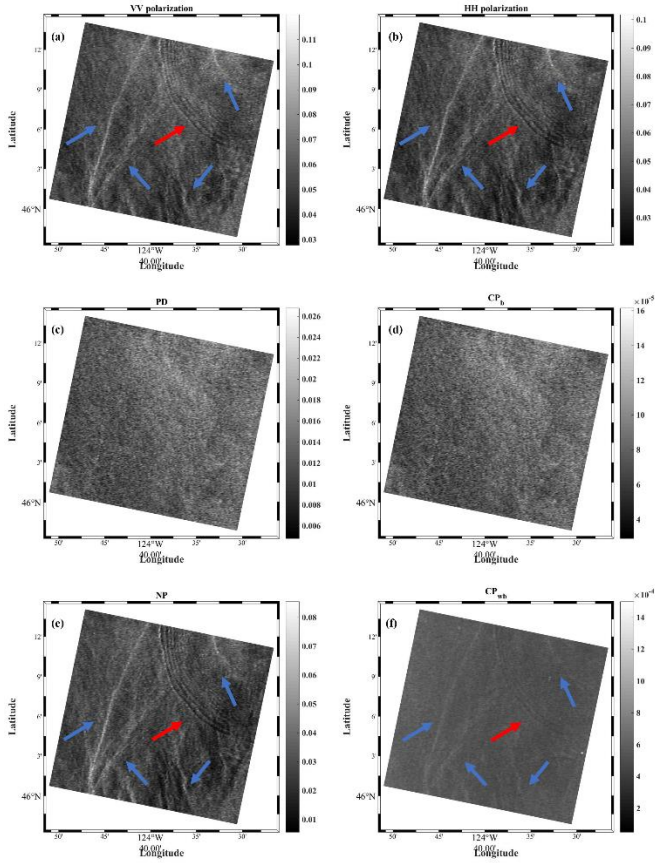

Fig. 1. RADARSAT-2 SAR image of a coastal area in the east coasts of the USA acquired at 14:35 UTC on August 15, 2009 in terms of (a) VV-polarization, i.e., σ_0^{vv}(in linear units); (b) HH-polarization, i.e., σ_0^{hh}; (c) PD $\Delta\sigma = \sigma_0^{vv} - \sigma_0^{hh}$ (in linear units); (d) The contribution of Bragg scattering to cross-polarization radar signal, i.e., CP_b (in linear units); (e) The contribution of wave breaking to co-polarization radar signal, i.e., NP (in linear units); (f) The contribution of wave breaking to cross-polarization radar signal, i.e., CP_{wb} (in linear units); The blue and red arrows indicate manifestations of surface current signatures (front) and internal waves.

2.2 Model Approach

To interpret these observed SAR features, we follow model approach suggested in [2]. Following this approach, VV and HH NRCSs can be separated into two parts, associated with the polarized resonant Bragg scattering σ_{OB}^{pp} and the non-polarized (NP) radar returns from breaking waves σ_{wb}:

$$\sigma_0^{pp} = \sigma_{OB}^{pp} + \sigma_{wb} \quad (1)$$

Equations (1) for VV and HH can be solved to derive NP contribution, σ_{wb}, from dual co-polarized NRCS measurements:

$$\sigma_{wb} = \sigma_0^{vv} - \Delta\sigma_0/(1 - p_B) \quad (2)$$

where p_B is the polarization ratio for the two-scale Bragg scattering, ie.,

$$p_B = \sigma_{OB}^{hh}/\sigma_{OB}^{vv} \quad (3)$$

for the two-scale Bragg scattering, p_B is mostly governed by the local geometry and tilting effects.

2.3. Cross-polarized data

The same as (1) we split cross-polarization (CP; HV or/and VH) NRCS on two parts,

$$\sigma_0^{vh} = \sigma_{0B}^{vh} + \sigma_{0wb}^{vh} \quad (4)$$

where σ_{0B}^{vh} is TSM Bragg scattering prediction for CP. Within the frame of TSM model, CP-over-PD ratio, supported by regular surface, to the first order of the mean square slope (MSS), reads:

$$\left(\frac{CP}{PD}\right)_B \equiv \frac{\sigma_{0B}^{vh}}{\Delta\sigma_0} = \frac{|G_{vv} - G_{hh}|^2}{|G_{vv}|^2 - |G_{hh}|^2} \frac{s_n^2}{sin^2\,\theta} \quad (5)$$

$|G_{pp}|$ is the scattering coefficient, Relative contribution of wave breaking to CP, $\frac{\sigma_{0wb}^{vh}}{\sigma_0^{vh}}$, can easy be found from (4) and reads:

$$\frac{\sigma_{0wb}^{vh}}{\sigma_0^{vh}} = 1 - r_B \frac{\Delta\sigma_0}{\sigma_0^{vh}} \quad (6)$$

where $r_B = \left(\frac{CP}{PD}\right)_B$ is TSM prediction defined by (5). So, σ_{0wb}^{vh} can be shown as

$$\sigma_{0wb}^{vh} = \sigma_0^{vh} - r_B \Delta\sigma_0 \quad (7)$$

and for σ_{0B}^{vh},

$$\sigma_{0B}^{vh} = r_B \Delta\sigma_0 \quad (8)$$

Based on model (3), (7) and (8), the original co-polarized VV, HH and cross-polarized images can be thus transformed to new NP, σ_{0wb}^{vh} and σ_{0B}^{vh} images which possess information on very different radar scattering mechanisms, i.e., the polarized Bragg scattering provided by short fast-response wind waves and NP, σ_{0wb}^{vh} radar returns from breaking waves in a wide spectral range. Due to different sensitivity of short wind waves and wave breaking to various ocean phenomena, this set of new images can then serve as an effective tool for SAR data interpretation.

2.4. Scattering Mechanism Analysis

Fig. 1 suggests that the bright quasi-linear feature (associated with the surface currents manifestation) well visible in VV, HH, NP and σ_{0wb}^{vh} scenes are not distinguishable in the PD and σ_{0B}^{vh} scenes. This indicates that SAR signatures over oceanic fronts mostly result from enhanced wave breaking, which provide NP and σ_{0wb}^{vh} radar returns.

In Fig. 2, the same as Fig. 1, the bright quasi-linear feature well visible in VV, HH, NP and σ_{0wb}^{vh} scenes are not distinguishable in the PD and σ_{0B}^{vh} scenes. This means that local enhancement of wave breaking which caused by the current divergence in vicinity of the oceanic front has strong contributions to radar signals. We may interpret this front as the sea surface temperature front. Than spatial variability of PD signal can be associated with transformation of the atmospheric boundary layer over the SST front resulting in SST-correlated spatial changes in the near surface wind.

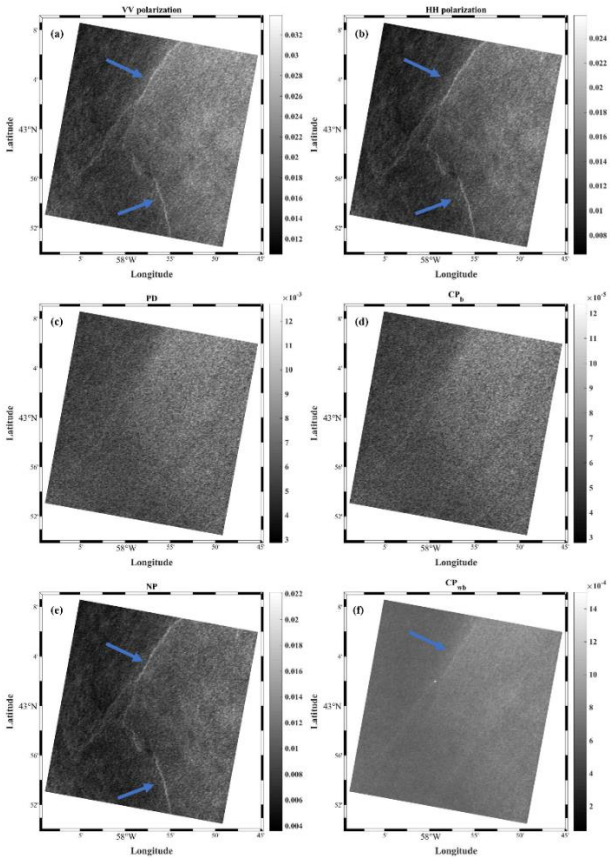

Fig. 2. RADARSAT-2 SAR image of a coastal area in the east coasts of the USA acquired at 14:35 UTC on August 15, 2009 in terms of (a) VV-polarization, i.e., σ_0^{vv}(in linear units); (b) HH-polarization, i.e., σ_0^{hh}; (c) PD $\Delta\sigma = \sigma_0^{vv} - \sigma_0^{hh}$ (in linear units); (d) The contribution of Bragg scattering to cross-polarization radar signal, i.e., CP_b (in linear units); (e) The contribution of wave breaking to co-polarization radar signal, i.e., NP (in linear units); (f) The contribution of wave breaking to cross-polarization radar signal, i.e., CP_{wb} (in linear units); The blue arrows indicate manifestations of surface current signatures (thermal front).

This wind speed variability is also well seen in NP field. In order to remove wind variability from NP signal and emphasize the remaining effect of wave breaking interactions with the surface currents, we decompose NP into two components, $\sigma_{wb} = \sigma_{wb}^{W} + \sigma_{wb}^{C}$ [6], where σ_{wb}^{W} is the wind driven NP component, and σ_{wb}^{C} is the NP deviation caused by wave current interactions. The part of NP anomalies caused by wave current interactions evaluated as

$$\sigma_{wb}^{C} = \sigma_{wb} - [\overline{\sigma_{wb}^{W}} + A(\Delta\sigma - \overline{\Delta\sigma})] \qquad (9)$$

where bars denote corresponding mean values and A is the regression coefficient, the result is shown in Fig. 3. Applying (9) essentially removes effects of wind variations (including wave-like patterns) from the original NP image (compare Fig. 2e and Fig. 3), thus emphasizing the bright frontal feature associated with the surface currents convergence.

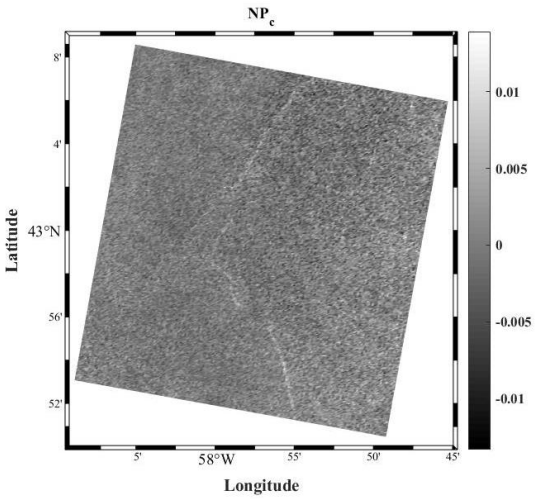

Fig. 3. NP variations caused by wave-current interaction (in linear units).

3. CONCLUSIONS

Dual co-polarization SAR data can thus provide a tool to distinguish between different mechanisms affecting ocean radar backscatter. NRCS difference between VV and HH copolarized data (PD image) enhances variability produced by the resonant scattering mechanism. As demonstrated, combination of VV, HH, CP and PD images can be then used to derive the NP and σ_{0wb}^{vh} components of the NRCS, essentially dominated by breaking waves. Since wave breakings are very sensitive to the nonuniform surface current, NP and σ_{0wb}^{vh} images shall reflect surface manifestations of sub- and mesoscale ocean currents.

4. ACKNOWLEDGMENTS

SF and BZ acknowledges support of National Key Research and Development Program of China under Grant 2016YFC1401001, National Science Foundation of China for Outstanding Young Scientist under Grant 41622604, and the Excellent Youth Science Foundation of Jiangsu Province under Grant BK2016090. VK and BC acknowledge support of Russian Science Foundation project no. 17-77-30019.

5. REFERENCES

[1] Kudryavtsev, V. N., B. Chapron, A. G. Myasoedov, F. Collard, and J. A. Johannessen (2013), On Dual Co-Polarized SAR Measurements of the Ocean Surface, *IEEE Geosci. Remote Sens. Lett*., 10, 761-765, doi: 10.1109/LGRS.2012.2222341.

[2] Kudryavtsev, V. N., I. Kozlov., B. Chapron, and J. A. Johannessen (2014), Quad-polarization SAR features of ocean currents, *J. Geophys. Rese., Oceans*., 119, 6046-6065, doi: 10.1002/2014JC010173.